Eco-evolutionary processes underlying early warning signals of population declines

Gaurav Baruah[1], Christopher F. Clements[1,2], Arpat Ozgul[1]

[1] Department of Evolutionary Biology and Environmental studies, University of Zurich, Winterthurerstrasse 30, 4055 Zurich

[2] School of Biosciences, University of Melbourne, Parkville VIC 3052, Australia
Melbourne

Corresponding author: Gaurav Baruah
Email: gaurav.baruah@ieu.uzh.ch

Abstract

Environmental change can impact the stability of a population and cause a rapid decline in abundance. Abundance-based early warning signals have been proposed to predict such declines, but these have been shown to have limited success, leading to the development of warning signals based on the distribution of fitness-related phenotypic traits such as body size. The dynamics of such traits in response to external environmental perturbations are controlled by a range of underlying factors such as reproductive rate, genetic variation, and plasticity. However, it remains unknown how such ecological and evolutionary factors affect the stability landscape of populations and the detectability of abundance and trait-based warning signals of population decline. Here, we apply a trait-based demographic approach and investigate both trait and population dynamics in response to gradual changes in the environment. We explore a range of ecological and evolutionary constraints under which the stability of a population may be affected. We show both analytically and with model-based simulations that strength of abundance-based early warning signals is significantly affected by ecological and evolutionary factors. Finally, we show that a unified approach, combining trait- and abundance-based information, significantly improves our ability to predict population declines.

1. Introduction

Projected anthropogenic influences on earth systems will continue to increase over the next 100 years and will significantly change the earth's biota (Mora et al. 2013). The impact of anthropogenic forcing can often bring natural populations and complex ecosystems into the region of tipping points (Wissel 1984; Scheffer et al. 2001; Scheffer et al. 2012), This point represents the threshold at which any slight increase in pressure or stochastic fluctuation can cause a transition from a stable state to an alternative state – exemplified by the collapse of populations (Frank et al. 2011) or change in ecosystem functions (Jackson et al. 2001; Frank et al. 2011). Predicting such transitions are thus critical if we are to mitigate the effects of human pressures and minimize the loss of biodiversity (Cardillo et al. 2005; Thomas et al. 2004). These transitions are however difficult to predict (Clements et al. 2015; Boettiger & Hastings 2013; Clements & Ozgul 2018).

One suite of methods, which may achieve this, are early warning signals derived from dynamic systems theory (van Nes & Scheffer 2007; M. Scheffer et al. 2009). Such methods assume that a dynamical system, for example a biological population, that is under increasing continuous external pressure, will show a property called critical slowing down (CSD) as it approaches a tipping point, whereby the system takes longer to return to its original state after a perturbation (Wissel 1984; Dakos et al. 2008; Scheffer et al. 2009; Strogatz 1994). The occurrence of CSD is a direct implication of the dominant eigenvalue of the system approaching zero (for continuous dynamical system) (van Nes & Scheffer 2007) or 1 (for a discrete dynamical system) (Krko ek & Drake 2014). As a direct consequence of CSD, statistical moments embedded within abundance time-series data, particularly variance and autocorrelation will show marked increase over time. These two indicators are the prominent abundance-based statistical metrics, and, along with various other metrics (Dakos et al. 2012; C. Boettiger & Hastings 2012;

Clements & Ozgul 2016; Clements & Ozgul 2018; Drake & Griffen 2010), are commonly known as early warning signals (EWS) or leading indicators.

Changes in autocorrelation and variance are measures of the stability of a system, derived from theory of alternative stable states (Wissel 1984; Clements & Ozgul 2018). Holling's (1973) fundamental work on stability and resilience laid the foundation for future work on deriving stability criteria for systems with alternative equilibrium states. Stability of a dynamical system can be characterized by the classic ball-in-cup diagram (Holling 1973; Nolting & Abbott 2015; Clements & Ozgul 2018), where the 'ball' represents the state of the system and the 'cup' represents the potential energy landscape. The stability of the system is thus quantified by the depth of the energy landscape, and resilience by the size of the cup (Villa Martín et al. 2015; Dai et al. 2015; Clements & Ozgul 2018). In response to continuous exogenous pressure, the system loses resilience (for example, decline in population numbers) and the energy landscape shrinks. Concurrent with the shrinkage of the landscape, there is also a decrease in the depth of the 'ball-in-cup' landscape signaling the loss in stability. It is this loss in stability, which statistical EWSs such as variance and autocorrelation measure as an alternative for loss of global resilience of the system (Clements and Ozgul 2018). The shape of the ball-in-cup landscape thus determines the dynamics of the state variable in response to an exogenous environmental change (Beisner et al. 2003).

However, the shape of the 'ball-in-cup' landscape can be changed not only by exogenous pressures, but can also be altered by intrinsic factors associated with the system's dynamics (Beisner et al. 2003). Changes in these intrinsic factors might alter the location of an equilibrium state, or destabilize the current state, causing the system to arrive at a point closer to the other alternative state (see Fig. 1). For a biological population, the state of the population will be characterized by its current abundance. Responses of this state variable (abundance) to an exogenous environmental pressure will be a combination of ecological and evolutionary responses controlled by factors such as

genetic variation or plasticity (Price et al. 2003; Gienapp et al. 2008; Ozgul et al. 2010). For example, plastic responses to fluctuating changes in the exogenous environment are usually fast which consequently stabilizes population fluctuations (Reed et al. 2010). However, if the environment keeps on changing, the population might not only deplete its plastic capacity but also its standing genetic variation, which in turn leads to its eventual decline. Further, such a decline would also be conditional on the population's reproductive rate, with higher reproductive rate leading to a slower decline (Juan-Jordá et al. 2015). In addition, due to continuous changes in the exogenous environment, selection pressures can subsequently increase leading to contemporary evolution (Yoshida et al. 2003). Adaptive evolution would then depend on the amount of genetic variation present in the population with higher variation leading to faster evolution, which can either stabilize or destabilize population dynamics (Sanchez & Gore 2013; Cortez 2016). Since the dynamics of a population in response to an exogenous pressure is determined by the shape of its potential energy landscape (Beisner et al. 2003), it is thus highly probable that changes in these factors namely plasticity, genetic variation, and reproductive rate have the capacity to influence the shape of the ball-in-cup landscape. In turn, given that EWS are stability measures derived from alternative stable states theory (Beisner et al. 2003; Scheffer et al. 2009; Clements & Ozgul 2018), it is very likely that strength in EWS and hence predictability of population decline might also be affected by these factors.

The EWSs described above are phenomenological signals which require very few assumptions about the mechanistic processes driving system dynamics, which makes them applicable to a wide variety of systems (Wissel 1984; Scheffer et al. 2009; Clements et al. 2017; Clements and Ozgul 2018; Jarvis et al. 2016; Dutta, Sharma, and Abbott 2018). However, such statistical tools have a multitude of issues associated with it, for example- low signal to noise ratio and the requirement of high-quality time-series data (Clements et al. 2015). This had led to the development of alternatives like

maximum likelihood-based (Boettiger & Hastings 2012; Brock & Carpenter 2012) and generalized system-specific modelling approaches (Lade & Gross 2012). However, for many natural and ecological systems specific models might not be easily available, and a generic EWS approach then becomes necessary.

Abundance-based measures of the stability of an ecological system might not be the only indicators of a population being forced by an external environment (Clements & Ozgul 2016) . Phenotypic traits, such as body size, is one of the important traits that determines the fate of individuals as well as dynamics of population, and thus can provide crucial information regarding the current state of the population (Clements and Ozgul 2016b; Ozgul et al. 2014; Spanbauer et al. 2016). Recently, Clements & Ozgul (2016) showed, using data from experimental microcosms, that including body size information with EWS could significantly improve the predictive accuracy of population collapse. Such trait-based signals, have been further shown to be present in the historic collapses of whale populations (Clements et al. 2017). However, extensive research on the efficacy of such signals in comparison to abundance-based EWS is still in its infancy (Clements & Ozgul 2018).

In this paper, we used a quantitative genetics framework to simulate the dynamics of a population in response to gradual environmental change. We track both the population dynamics and trait distribution until the simulated population collapses. We show that this particular model exhibits critical slowing down behavior and hence is expected to show EWS (van Nes and Scheffer 2007). We then assess whether genetic variation, plasticity in the trait, and net reproductive rate alter the ball-in-cup landscape (stability landscape) and consequently the strength in EWS. In addition, we assess the efficacy of trait-based EWS in comparison with abundance-based EWS and reiterate the ability of trait-based signals in accurately informing population collapses.

2. Materials and Methods

2.1 Mathematical model:

We model the joint dynamics of quantitative trait evolution and population size under density dependent regulation via the effects of selection (Gomulkiewicz & Holt 1995; Chevin et al. 2010; Chevin & Lande 2010) . We consider a population that has discrete generations where individuals have fitness that is determined by a single quantitative trait z under stabilizing selection with linear reaction norms (Gavrilets & Scheiner 1993). The phenotype of an individual *i* in this finite population before selection is given by:

$$z_{i,t} = a_{i,t} + bu_t + \epsilon \qquad (1)$$

where a is the breeding value of the individual i. The breeding value is normally distributed with mean $\overline{a}$ and additive genetic variance σ_a^2, and ϵ is the residual component with mean 0 and variance σ_ϵ^2. The slope b in our model is constant meaning that plasticity in the trait cannot evolve. We model an environment that determines the optimal phenotypic value θ_t for the primary phenotype z_t and also cues the plastic response. The optimal phenotype. θ_t, is assumed to be linearly dependent on the environment E that selects for a particular phenotypic value such that, $\theta_t = BE_t$.

We included stochasticity in the environment E_t as a Gaussian white noise process. The optimal phenotype hence fluctuates as E_t fluctuates over a mean value. As in Reed et al. (2010), the environmental cue u and the optimal phenotype θ are drawn from a bivariate normal distribution at each generation t with equal variances. The covariance of u and θ is given by $\sigma_{\theta,u} = \xi\sigma_\theta\sigma_u$ where ξ is the correlation between θ and the cue u. The environmental cue u is drawn from the distribution with its mean value U_t over time given by:

$$U_t = \begin{cases} 0 & , t < t_{500} \\ 1 - c\frac{t}{500} & , \ t \geq t_{500} \end{cases} \qquad (2)$$

And for optimal phenotype θ is drawn from the bivariate distribution with mean value given by:

$$\theta_t = BE_t = \begin{cases} 0 & , t < t_{500} \\ B - B\frac{t}{500} & , t \geq t_{500} \end{cases} \quad (3)$$

We assumed that variances in the cue and the optimum are equal. This mimics the situation, for instance, when variation in food availability is correlated with inter annual variation in snow melt (Vuren & Armitage 1991). ξ determines predictability of the environment such that ξ = 1 means the environmental cue is correlated with the optimum phenotype in a way that the plastic response tracks the optimum environment perfectly. In such a case, the strength in plastic response of the trait will be determined by *b.*

The mean phenotype at any generation t is then: $\bar{z} = \bar{a} + bu_t$ and has variance: $\sigma_z^2 = \sigma_a^2 + \sigma_\epsilon$ (We consider $\sigma_\epsilon \approx 0, \sigma_z^2 = \sigma_a^2$). Without loss of generality, at the reference environment, i.e., $u_t = 0$, the phenotype is assumed to be at its optimum value. Each individual in this population has a net reproductive fitness of R_0 that is under density-dependent regulation. The primary trait z determines its reproductive fitness in the sense that:

$$R(z) = R_0^{(1-\frac{f(N_t)}{f(K)})} W(z) \quad (4)$$

where, $\frac{f(N_t)}{f(K)}$ is a density-dependent function and W(z) is the Gaussian stabilizing fitness function :

$$W(\mathrm{z}, \theta) = e^{-(\mathrm{z}-\theta)^2/2\sigma_w^2} \quad (5)$$

If the primary trait z is far from its optimum phenotype θ then its fitness will decline depending on the width σ_w^2 of the fitness function $W(\mathrm{z}, \theta)$, which signifies the strength

of selection. Assuming that the phenotypic distribution to be normal *p(z)*, the average reproductive fitness of the population will be

$$\bar{R} = R_0^{\left(1-\frac{f(N_t)}{f(K)}\right)} \int W(z)p(z)dz \qquad (6)$$

If time *t* is in generations, then population size at *t+1* is

$$N_{t+1} = N_t \bar{R} \qquad (7)$$

And the dynamics of mean phenotypic value is:

$$\bar{z}_{t+1} = \bar{a}_t + \sigma_a^2 \frac{\partial ln\overline{W}}{\partial \bar{a}} + bu_t \qquad (8)$$

where, $\overline{W} = \int W(z)p(z)dz = \sqrt{\frac{\sigma_w^2}{\sigma_z^2+\sigma_w^2}}\, e^{-(\overline{z_t}-\theta_t)^2/2(\sigma_w^2+\sigma_z^2)}$.

The above model is based on the infinitesimal quantitative genetic model (Falconer & Mackay 1996).

2.2 Stability landscape and effective potential:

One approach to quantifying stability which is also fundamental to dynamical systems with alternative stable states is the 'ball-in-cup' analogy (Haydon 2003; Villa Martín et al. 2015). The different states of the dynamical system can be represented by a landscape and the state of the population at a particular moment by a ball in that landscape. The landscape of the dynamical system can be represented by an effective potential $V(N)$ (Villa Martín et al. 2015; Beisner et al. 2003). If the dynamical system can be represented by $\frac{dn}{dt} = g(n)$, then $V(n) = -\int g(n)dn$. For our dynamical system, $g(n) = \log\left(R_0^{\left(1-\frac{n}{k}+\beta-\gamma\right)}\right)$. Here *n* is the state of the system, which in our case is the population size. The effective potential of our dynamical system is then (supplementary 4):

$$V(n) = -\left(rn - \frac{\frac{r}{k}n^2}{2} + \beta rn - \gamma rn \right)$$

$$= \left(rn - \frac{\frac{r}{k}n^2}{2} + \frac{\log\left(\frac{\sqrt{(\sigma_w^2)}}{\sqrt{(\sigma_w^2 + \sigma_z^2}}\right)}{\log(R_0)} rn - \frac{(\bar{a} + bu_t - \theta_t)^2}{(R_0(\sigma_w^2 + \sigma_z^2))} rn \right) \quad (9)$$

It is evident from the above equation (9) that the effective potential function is dependent on three parameters: r, β, γ, where r = log(R_0); $\beta = \frac{\log\left(\frac{\sqrt{(\sigma_w^2)}}{\sqrt{(\sigma_w^2+\sigma_z^2}}\right)}{\log(R_0)}$; $\gamma = \frac{(\bar{z}-\theta_t)^2}{(R_0(\sigma_w^2+\sigma_z^2))}$; n = log(N) ; k= log(K).

2.3 Equilibria and eigenvalues of the model:

The extinction equilibrium for the model is at $N^* = 0$ and the positive equilibrium for the model is at $N^* = K + \beta K - \gamma K$, where $\gamma = \frac{(\bar{z}-\theta_t)^2}{(R_0(\sigma_w^2+\sigma_z^2))}$; $\beta = \log\left(\frac{\sqrt{(\sigma_w^2)}}{\sqrt{(\sigma_w^2+\sigma_z^2}}\right) / \log(R_0)$ (see supplementary 1). Stability of the two equilibria are based on their corresponding eigenvalues, $\lambda = \frac{\partial}{\partial N} f(N)|_{N=N^*}$. Equilibria will be stable if magnitude of $\lambda < 1$ and unstable if magnitude of $\lambda > 1$ (Supplementary 1). Local stability analysis gives for the extinction equilibrium N* = 0, $\lambda_1 = R_0^{1+\beta-\gamma}$ and for positive equilibrium $N^* = K + \beta K - \gamma K$, $\lambda_2 = 1 - (1 + \beta - \gamma) log R_0$. Thus, the extinction equilibrium N* = 0, is always unstable since $\lambda_1 = R_0^{1+\beta-\gamma} > 1$ whenever $R_0 > 1$. On the other hand, the positive equilibrium $N^* = K + \beta K - \gamma K$ is stable conditional on the forcing parameter $\gamma = \frac{(\bar{z}-\theta_t)^2}{(R_0(\sigma_w^2+\sigma_z^2))}$ and $R_0 > 1$. Assuming that the phenotype is at its optimum ($\bar{z} = \theta$) i.e., $\gamma = 0$, then for $R_0 > 1$ the positive equilibrium is stable due to $\lambda_2 = 1 - (1 + \beta - \gamma) log R_0 < 1$. But as the forcing parameter $\gamma = \frac{(\bar{z}-\theta_t)^2}{(R_0(\sigma_w^2+\sigma_z^2))}$ increases over time (due to

θ_t shifting and the phenotype lagging behind), λ_2 slowly approaches 1 and the positive equilibrium which is $N^* = K + \beta K - \gamma K$ is initially stable but becomes unstable once λ_2 reaches 1. This happens when increases in the forcing parameter γ or increases in maladaptation causes average population growth rate $\bar{R}$ (4) also to reach 1. Once this happens, the extinction equilibrium then becomes stable at $\bar{R} = 1$ and the two equilibrium exchange stability at $\bar{R} = 1$. This is the definition of transcritical bifurcation. Moreover, as $\bar{R}$ approaches 1, the magnitude of λ_2 becomes larger and the recovery rate from external perturbation becomes slower (see supplementary 1 and 2). This indicates that there is CSD. λ_2 is directly related to return time, from which indicators like autocorrelation and standard deviation can be calculated (supplementary 2).

2.4 Simulations of population collapse

To complement our theoretical findings we did simulations and forced the populations to collapse by increasing the rate of change in the environment E_t. We chose a rate of change in the environment θ_t in a way that populations collapsed regardless of any combination of parameter values. This was done by setting B =60 in (3) in all of our simulations. Environmental change was introduced at time point t = 500, after populations have reached their carrying capacity. In all of our simulations, environmental predictability was high at $\xi = 1$. For each parameter value of a factor (genetic variation, plasticity, net reproductive rate) we did 200 independent simulations of population collapse. For each population time series, we first estimated the bifurcation point by fitting GAMS to $\frac{N_{t+1}}{N_t}$ over time t. $\frac{N_{t+1}}{N_t} < 1$ is then our estimated bifurcation point in our simulations.

2.4.1 Abundance-based EWS

For abundance-based EWS analyses, the length of the time-series used was of the same length for each factor in question. For each parameter value of each factor in question, we used time-series data to the estimated bifurcation point. We discarded time-series

269 data after the bifurcation point. The bifurcation point in the time-series however varied
270 due to different levels of parameter values for a factor in question, resulting in a range of
271 abundance time-series lengths (from as low as 30 to 110 time points from t = 500 where
272 the optimum environments shifts). Hence due to the possible effect of length of time-
273 series on strength of EWS of population collapse, we standardized the time-series length
274 such that each population time-series analyzed for EWS had the same length. We then
275 applied generic EWS of population collapse by using the *earlywarnings* package in R. We
276 focused our analysis on two specific indicators namely autocorrelation at the first-lag
277 (AR1) and standard deviation (SD) as most of the other indicators – such as first-order
278 autoregressive coefficient or coefficient of variation – could be theoretically derived
279 from these parameters (Dakos et al. 2012). The two indicators AR1 and SD were
280 calculated using a predefined sliding window, typically 50% of the abundance time-
281 series being analyzed. We normalized the leading indicators so that it would be easier
282 to incorporate information from phenotypic traits later in our analyses. We used
283 Gaussian detrending to remove any trend in the abundance time-series and used
284 Kendall's Tau correlation coefficients of the indicators prior to the estimated bifurcation
285 point as an indicator of an approaching collapse. Strong positive correlations of the
286 statistical indicators (SD and AR1) with time would indicate an approaching population
287 collapse which would be evident in a higher value of Kendall's Tau coefficient (Dakos et
288 al. 2012).

289 *2.4.2 Trait-based EWS*

290 To evaluate the efficacy of trait-based EWS (Clements & Ozgul 2016), information from
291 mean phenotypic trait was incorporated with the leading indicators in an additive
292 manner. To include information from average phenotypic value, we first normalized the
293 phenotypic time-series. The length of the phenotypic time-series that was used was the
294 same as the corresponding abundance time-series. Standardized EWS such as standard

295 deviation and auto-correlation (SD, AR1) were added additively with standardized mean
296 phenotypic time series to quantitatively create trait-based signals. We evaluated three
297 trait-based EWS metrics namely *AR1+trait, AR1+SD+trait, SD+trait* and compared how
298 the metrics that included information from the mean phenotype improved predictability
299 of population collapse when compared with the standardized abundance-based EWS
300 like *AR1, SD, AR1+SD*. We quantified Kendall's Tau correlation coefficient as an indicator
301 for strength of predictability of population collapse.

302 *2.4.3 Adaptive plasticity:* To assess the role of adaptive plasticity *b*, we simulated 200
303 replicate population collapses for each parameter value of *b,* which ranged from low to
304 high: 0.02, 0.06, 0.1, 0.2, 0.4, and 0.6. While we varied plasticity, we fixed $\sigma_a^2 = 0.2$, and
305 R_0 at 1.2. The width of the fitness function determines the strength of selection in the
306 trait. We fixed the width of the fitness function at $\sigma_w^2 = 25$, which would indicate
307 medium strength in selection. Usually, $\sigma_w^2 = 50$ would indicate weak strength in
308 selection and $\sigma_w^2 = 5$ would indicate strong selection (Chevin and Lande 2010).

309 *2.4.4 Genetic variation:* The levels of genetic variation σ_a^2 used for the simulations of
310 population collapse are 0.02, 0.06, 0.1, 0.2,0.3,0.5, 0.6. Adaptive plasticity *b*, net
311 reproductive rate R_0 and σ_w^2 were kept at 0.2, 1.2 and 25 respectively.
312 We also did simulations where we relaxed the assumption of genetic variation (σ_a^2)
313 remaining constant during population collapses. For details see supplementary 5.
314

315 *2.4.5 Net reproductive rate:* To assess the role R_0, we simulated 200 replicate population
316 collapses. The levels of R_0 used for the simulations of population collapse were 1.1, 1.2,
317 1.3, 1.4, and 1.5. Adaptive plasticity *b*, genetic variation σ_a^2 and σ_w^2, were kept at 0.2, 0.2
318 and 25 respectively.

319 **3. Results**

320 *3.1 Effective potential*

3.1.1 Strength in plasticity

The term $\gamma = \frac{(\bar{z}-\theta_t)^2}{(R_0(\sigma_w^2+\sigma_z^2))}$ in equation (9) is the evolutionary lag due to maladaptation of the mean phenotype with the optimum (Lande 2009). The effective potential becomes narrower with increasing strength in plasticity and consequentially increases stability, i.e., the potential function becomes more negative (Fig. 2). Since return time and stability are inversely related (Dai et al. 2015), return time decreases with increasing strength in plasticity (Supplementary 2, Fig. S1). In other words, the population quickly recovers with every perturbation if strength in plasticity is high.

3.1.2 Genetic variation

The mean phenotype has variance of $\sigma_z^2 = \sigma_a^2 + \sigma_\epsilon$. Assuming residual component σ_ϵ to be zero, phenotypic variance is then equal to additive genetic variance, $\sigma_z^2 = \sigma_a^2$. Inspection of the equation (9) reveals that high additive genetic variance causes the effective potential to be more positive when compared with low σ_a^2 and consequently decreases stability, i.e., the effective potential becomes less negative (Fig. 2; the more negative the effective potential, more stable the population is). Loss of stability and effective potential energy is higher for populations with low genetic variance whenever they are forced to collapse compared to populations with high genetic variance (Fig. 2, supplementary 3). Further, return time also increases with increasing additive genetic variance (supplementary 2, Fig. S1).

3.1.3 Net reproductive rate

From equation (9), we also see that higher values of R_0 lead to higher stability and narrow potential curve for a given state of the population (Fig. 2). Loss in stability is more when R_0 is higher for the same rate of change in the environmental change when compared with a lower R_0. Further, return time also decreases with increasing R_0 (supplementary 2, Fig. S1).

3.2 Simulations of population collapse: abundance-based EWS

347 *3.2.1 Strength in plasticity*

348 The strength of EWSs of population collapse (Kendall's Tau value) was much higher in
349 populations which had high adaptive plasticity ***b*** = 0.6 (Fig. 3a, d) when compared with
350 populations with low adaptive plasticity.

351 *3.2.2 Genetic variation*

352 Our model simulations showed that genetic variation altered the detectability of
353 population collapse for the same rate of environmental change (Fig. 3b, 3e). Higher
354 genetic variation in the population led to slight decrease in detectability of population
355 collapse than in populations with lower genetic variation.

356 *3.2.3 Net reproductive rate*

357 Strength in EWS of populations collapse was significantly altered by net reproductive
358 rate. Strength in EWS was lower in populations with lower R_0 when compared with
359 higher R_0 (Fig. 3c, 3f). Both the leading indicators SD and AR1 showed similar behavior
360 in this aspect (Fig. 3c, 3f), but Kendall's tau value of SD showed significant increases in
361 strength as net reproductive rate increased.

362 *3.3 Simulations of population collapse: trait-based EWS*

363 Including information from trait value alongside abundance-based EWS significantly
364 improved the strength of EWS of population collapse (Fig. 4, Fig S8-S9). In principle, *AR1*
365 was the least efficient of all the signals compared. However, when trait information was
366 included with *AR1*, strength in trait-based *AR1 (trait+AR1)* improved significantly
367 (Fig.4). Overall, the Kendall's Tau value of *SD+trait* was relatively higher than all the
368 other trait-based and abundance-based EWS. The extent of the distribution of Kendall's
369 tau values of *SD+trait* signal was much lower than that of just *SD* (Fig. 4). This was
370 consistent across all the factors analyzed such as genetic variation, plasticity (Fig.4, Fig.
371 S8-S9).

372 **4. Discussion**

373 The early detection of population collapse with the help of EWS provides a unique tool
374 to highlight conservation efforts to a population approaching an impending transition.
375 These tools are relatively simple, easy to use, as they only require state-based data like
376 abundance and hence are applicable to a variety of ecological systems. However, we
377 show here that factors intrinsic to a population in question such as genetic variation,
378 plasticity or net reproductive rate could significantly alter stability of a population as
379 well as strength in EWS of population decline.

380 The detectability of EWSs is dependent not only on the relation between stability and
381 resilience but is also determined by a variety of factors including sampling frequency,
382 and the strength and type of external forcing (Dai, Korolev, and Gore 2015; Clements et
383 al. 2015a; Clements and Ozgul 2016). Here we add to this body of knowledge by
384 demonstrating that the effective potential of a system can also be altered by intrinsic
385 factors such as genetic variation, plasticity and net reproductive rate. These changes to
386 the effective potential in turn led to stronger EWS being observed, when changes in the
387 external optimum caused a population to lose significant amount of potential energy. In
388 other words, stronger EWSs would be observed whenever a population is forced to
389 move from a deeper point in the potential energy curve (more stable) to its tipping point
390 compared to another population, which is lying on a shallower potential (less stable).
391 Our findings also suggested that the utility of EWS was strongly determined by factors
392 that are intrinsic to a population such as genetic variation, net reproductive rate and
393 plasticity.

394 Higher strength in plasticity in the phenotype significantly affected the detectability of
395 population collapse (Fig. 2). Strength in plasticity altered the response and the dynamics
396 of a population to changes in the external environment. When plasticity was high the
397 response of the phenotype tracked the environment perfectly causing the population to

398 stabilize in response to fluctuating changes in the environment (Fig. S3) (Reed et al.
399 2011; Charmantier et al. 2008). The stability of a population is also reflected in short
400 return time to equilibrium (van Nes & Scheffer 2007). This was true for the case where
401 the strength in plasticity was high (Fig. S1). Moreover, the basin of attraction for a highly
402 plastic population was deeper when compared to a less plastic population, which was
403 shallower. To push a highly plastic population from the deepest point in its basin of
404 attraction to the tipping point, the energy loss would be more, compared to a less plastic
405 population which was lying in a much shallower basin. The loss in energy from driving
406 the highly plastic population from the deepest point to its tipping point was reflected in
407 stronger EWS when one compared it with another less plastic population. Consequently,
408 for the same rate of change in the environment, differences in Kendall's Tau values for
409 different values of plasticity was observed, with higher values of plasticity leading to
410 stronger EWS of population collapse.

411 Similarly, the effective potential of our dynamical system was also altered by genetic
412 variation (Fig. 2), with higher genetic variation leading to a shallower stability landscape
413 than that of a population with lower genetic variation. High additive genetic variance
414 created what was called a 'genetic load' that lowered the overall population growth rate
415 (Lande 1976; Lande and Shannon 1996; Chevin, Lande, and Mace 2010). This was due to
416 stabilizing selection acting on the mean phenotype. Due to this genetic load caused by
417 high additive genetic variance, population growth rate at equilibrium was lower causing
418 the effective potential to be closer towards the tipping point compared to another
419 population having a lower genetic variation. Hence for the same rate of external
420 environmental change, the loss of potential was different when one compared a
421 population with high genetic variation to that with low genetic variation. As a result, the
422 performance of EWS was affected with lower detectability of population collapse when
423 there was higher genetic variation (Fig. 3). This result however did not mean that
424 genetic variation was detrimental for long-term population persistence. Time to

extinction was however longer for populations with higher genetic variation when compared with a population which had a lower genetic variation in the trait (Fig S2)(Robinson et al. 2013; Yvonne & Hoffmann 2009). High genetic variation is necessary for rapid adaptation via genetic evolution, which then aids in evolutionary rescue (Chevin & Lande 2010). However our model simulations and analyses of EWS were mainly focused on short transient dynamics after the start of the external optimum change. Further, due to continuous and fast rate of environmental deterioration, adaptation or evolutionary rescue by genetic evolution (Lande 1976; Lande 2009; Chevin and Lande 2010) was not possible in our model and the populations eventually collapsed.

Decreasing population size in response to environmental deterioration and directional selection acting towards a mean phenotype could both lead to depletion of additive genetic variance (Barton & Keightley 2002). We took this account in our simulations by following a framework developed in (Bürger 2000). Using this framework to simulate population collapse we compared strength of EWS between two cases: 1) when there was decrease in genetic variation over time due to environmental deterioration and, 2) when genetic variation remained constant over time, however the results were largely similar (See Fig S6). Depletion of genetic variation over time did not affect the strength of EWS compared with when genetic variation remained constant.

Net reproductive rate also had a significant affect on the stability of populations and detectability of EWS of population collapse. Populations with a lower net reproductive rate declined steeply and earlier than populations with higher net reproductive rate for the same rate of external environmental change (Fig. S5). Higher net reproductive rate buffered the population from declining immediately after the environment shifted when compared to a population with lower reproductive rate (Juan-Jordá et al. 2015). Consequently, for the same rate of change in the external optimum environment,

451 populations with lower reproductive rate recovered slowly due to a wide basin of
452 attraction than populations with higher net reproductive rate (Fig. 2, Fig. S1) and hence
453 strength in EWS was more pronounced in the latter.

454 Our modeling results suggested that including fitness-related trait information could
455 significantly improve the strength in EWS of population collapse. Trait-based EWS
456 (*SD+trait*) produced the strongest signal. Inclusion of phenotypic trait information
457 alongside the leading indicators produced less distributed, consistent and stronger
458 Kendall's tau values compared to the generic abundance-based EWS (Fig. 4, Fig S8-S9).
459 In all the different biological factors examined in our study the *SD+trait* metric
460 performed the best overall. In response to a directional change in the external optimum
461 environment, shift in the mean phenotypic trait occurred over time even if there were
462 not significant increases in either AR1 or SD. Furthermore, including information from
463 the mean phenotype alongside EWS statistics would depend not only on whether the
464 mean phenotype responded to the external forcing but also on the nature of the external
465 environmental forcing itself (Clements & Ozgul 2016). Nevertheless, body size is a
466 candidate to be included with the leading indicators (Clements & Ozgul 2016). Shifts in
467 body size have previously been shown to occur before population collapse in whales,
468 with true positive EWS being detectable earlier when information from the body size
469 was included in the EWS (Clements et al. 2017).

470 In conclusion, we showed that predictability of population collapse was affected by
471 factors intrinsic to a population like genetic variation, strength in adaptive plasticity and
472 net reproductive rate. Changes in these factors can not only alter the underlying
473 phenotypic and population dynamics, but also the potential energy landscape.
474 Consequently, due to the alteration of the potential energy landscape, the detectability
475 of EWS was severely hampered. However, if information from fitness-related trait was
476 incorporated with EWS, the strength in predicting population collapses increased

significantly. Our results add to the body of evidence suggesting that the inclusion of trait dynamic information alongside the generic EWS should provide more accurate forecasts of the future state of biological systems.

Author's Contribution: GB designed the study, analyzed the model and did the simulations with feedback from CC and AO. All the authors contributed to writing the paper.

REFERENCES

Barton, N.H. & Keightley, P.D., 2002. Understanding quantitative genetic variation. *Nature reviews. Genetics*, 3(1), pp.11–21.

Beisner, B., Haydon, D. & Cuddington, K., 2003. Alternative stable states in ecology. *Frontiers in Ecology and the Environment*, 1(7), pp.376–382. Available at: https://esajournals.onlinelibrary.wiley.com/doi/10.1890/1540-9295%282003%29001%5B0376%3AASSIE%5D2.0.CO%3B2 [Accessed May 22, 2018].

Boettiger, C. & Hastings, A., 2013. No early warning signals for stochastic transitions: insights from large deviation theory. *Proceedings of the Royal Society, Series B*, 280(1766), p.20131372. Available at: http://www.ncbi.nlm.nih.gov/pubmed/23843397.

Boettiger, C. & Hastings, A., 2012. Quantifying limits to detection of early warning for critical transitions. *Journal of the Royal Society, Interface / the Royal Society*.

Boettiger & Hastings, 2012. Quantifying limits to detection of early warning for critical transitions. *Journal of The Royal Society Interface*, 9(75), pp.2527–2539.

Brock, W.A. & Carpenter, S.R., 2012. Early Warnings of Regime Shift When the Ecosystem Structure Is Unknown. *PLoS ONE*, 7(9).

Bürger, R. (Reinhard), 2000. *The mathematical theory of selection, recombination, and mutation*, Wiley.

Cardillo, M. et al., 2005. Multiple Causes of High Extinction Risk in Large Mammal Species. *Science*, 309(5738), pp.1239–1241. Available at: http://www.sciencemag.org/content/309/5738/1239%5Cnhttp://www.ncbi.nlm.nih.gov/pubmed/16037416%5Cnhttp://www.sciencemag.org/content/309/5738/1239.full%5Cnhttp://www.sciencemag.org/content/309/5738/1239.full.pdf.

Charmantier, A. et al., 2008. Adaptive phenotypic plasticity in response to climate change in a wild bird population. *Science (New York, N.Y.)*, 320(5877), pp.800–803.

Chevin, L.M., Lande, R. & Mace, G.M., 2010. Adaptation, plasticity and extintion in a changing enviroment: towards a predictive theory J. G. Kingsolver, ed. *PLoS biology*, 8(4), pp.1–8.

Chevin & Lande, 2010. When do adaptive plasticity and genetic evolution prevent extinction of a density-regulated population? *Evolution*, 64(4), pp.1143–1150.

Clements et al., 2017. Body size shifts and early warning signals precede the historic collapse of whale stocks. *Nature Ecology & Evolution*.

Clements et al., 2015. Factors Influencing the Detectability of Early Warning Signals of Population Collapse. *The American Naturalist*, 186(1), pp.50–58. Available at: http://www.jstor.org/stable/10.1086/681573%5Cnhttp://www.jstor.org/stable/pdf/10.1086/681573.pdf?acceptTC=true.

Clements, C.F. & Ozgul, A., 2016. Rate of forcing and the forecastability of critical

transitions. *Ecology and Evolution*, In press(April), pp.7787–7793.

Clements & Ozgul, A., 2016. Including trait-based early warning signals helps predict population collapse. *Nature Communications*, 7, p.10984. Available at: http://www.nature.com/doifinder/10.1038/ncomms10984.

Clements & Ozgul, A., 2018. Indicators of transitions in biological systems J. Metcalf, ed. *Ecology Letters*. Available at: http://doi.wiley.com/10.1111/ele.12948 [Accessed May 3, 2018].

Cortez, M.H., 2016. How the Magnitude of Prey Genetic Variation Alters Predator-Prey Eco-Evolutionary Dynamics. *The American naturalist*, 188(3), pp.329–41. Available at: https://www.journals.uchicago.edu/doi/10.1086/687393 [Accessed May 14, 2018].

Dai, L., Korolev, K.S. & Gore, J., 2015. Relation between stability and resilience determines the performance of early warning signals under different environmental drivers. *Proceedings of the National Academy of Sciences of the United States of America*, 112(32), pp.10056–61. Available at: http://www.ncbi.nlm.nih.gov/pubmed/26216946 [Accessed April 4, 2018].

Dakos, V. et al., 2012. Methods for detecting early warnings of critical transitions in time series illustrated using simulated ecological data. *PLoS ONE*, 7(7).

Dakos, V. et al., 2008. Slowing down as an early warning signal for abrupt climate change. *Proceedings of the National Academy of Sciences of the United States of America*, 105(38), pp.14308–12. Available at: http://www.pubmedcentral.nih.gov/articlerender.fcgi?artid=2567225&tool=pmcentrez&rendertype=abstract.

Dakos, V. & Bascompte, J., 2014. Critical slowing down as early warning for the onset of

collapse in mutualistic communities. *Proceedings of the National Academy of Sciences*, 111(49), pp.17546–17551. Available at: http://www.pnas.org/content/111/49/17546%5Cnhttp://www.ncbi.nlm.nih.gov/pubmed/25422412%5Cnhttp://www.pnas.org/content/111/49/17546.full.pdf.

Drake, J.M. & Griffen, B.D., 2010. Early warning signals of extinction in deteriorating environments. *Nature*, 467(7314), pp.456–9. Available at: http://dx.doi.org/10.1038/nature09389 [Accessed September 3, 2015].

Dutta, P.S., Sharma, Y. & Abbott, K.C., 2018. Robustness of early warning signals for catastrophic and non-catastrophic transitions. *Oikos*. Available at: http://doi.wiley.com/10.1111/oik.05172 [Accessed August 30, 2018].

Falconer, D.S. & Mackay, T.F.C., 1996. *Introduction to Quantitative Genetics (4th Edition)*, Available at: http://www.amazon.com/Introduction-Quantitative-Genetics-Douglas-Falconer/dp/0582243025.

Frank, K.T. et al., 2011. Transient dynamics of an altered large marine ecosystem. *Nature*, 477(7362), pp.86–9. Available at: http://www.ncbi.nlm.nih.gov/pubmed/21796120.

Gavrilets, S. & Scheiner, S.M., 1993. The genetics of phenotypic of reaction norm shape V . Evolution. *Journal of Evolutionary Biology*, 6(1), pp.31–48. Available at: http://onlinelibrary.wiley.com/doi/10.1046/j.1420-9101.1993.6010031.x/abstract.

Gienapp, P. et al., 2008. Climate change and evolution: Disentangling environmental and genetic responses. *Molecular Ecology*, 17(1), pp.167–178.

Gomulkiewicz, R. & Holt, R.D., 1995. When does evolution by natural selection prevent extinction? *Evolution*, 49(1), pp.201–207. Available at:

http://www.jstor.org/stable/10.2307/2410305%5Cnpapers2://publication/uuid/AF75FB13-CA45-471F-9595-604002DDAB20.

Haydon, D., 2003. Alternative stable states in ecology. *Frontiers in Ecology*.

Holling, C.S., 1973. Resilience and Stability of Ecological Systems. *Annual Review of Ecology and Systematics*, 4(1), pp.1–23. Available at: http://www.annualreviews.org/doi/10.1146/annurev.es.04.110173.000245 [Accessed May 22, 2018].

Jackson, J.B. et al., 2001. Historical overfishing and the recent collapse of coastal ecosystems. *Science (New York, N.Y.)*.

Jarvis, L. et al., 2016. Early warning signals detect critical impacts of experimental warming. *Ecology and Evolution*, 6(17), pp.6097–6106. Available at: http://doi.wiley.com/10.1002/ece3.2339 [Accessed August 30, 2018].

Juan-Jordá, M.J. et al., 2015. Population declines of tuna and relatives depend on their speed of life. *Proceedings of the Royal Society B: Biological Sciences*, 282(1811), p.20150322. Available at: http://rspb.royalsocietypublishing.org/lookup/doi/10.1098/rspb.2015.0322.

Krko ek, M. & Drake, J.M., 2014. On signals of phase transitions in salmon population dynamics. *Proceedings of the Royal Society B: Biological Sciences*, 281(1784), pp.20133221–20133221. Available at: http://rspb.royalsocietypublishing.org/cgi/doi/10.1098/rspb.2013.3221.

Lade, S.J. & Gross, T., 2012. Early warning signals for critical transitions: A generalized modeling approach. *PLoS Computational Biology*.

Lande, 2009. Adaptation to an extraordinary environment by evolution of phenotypic

plasticity and genetic assimilation. *Journal of Evolutionary Biology*, 22(7), pp.1435–1446.

Lande, R., 1976. NATURAL SELECTION AND RANDOM GENETIC DRIFT IN PHENOTYPIC EVOLUTION. *Evolution*, 30(2), pp.314–334. Available at: http://doi.wiley.com/10.1111/j.1558-5646.1976.tb00911.x [Accessed April 18, 2018].

Lande & Shannon, 1996. THE ROLE OF GENETIC VARIATION IN ADAPTATION AND POPULATION PERSISTENCE IN A CHANGING ENVIRONMENT. *Evolution*, 50(1), pp.434–437. Available at: http://doi.wiley.com/10.1111/j.1558-5646.1996.tb04504.x [Accessed April 18, 2018].

Mora, C. et al., 2013. Biotic and Human Vulnerability to Projected Changes in Ocean Biogeochemistry over the 21st Century. *PLoS Biology*.

van Nes, E.H. & Scheffer, M., 2007. Slow recovery from perturbations as a generic indicator of a nearby catastrophic shift. *The American naturalist*, 169(6), pp.738–747.

Nolting, B.C. & Abbott, K.C., 2015. Balls, cups, and quasi-potentials: quantifying stability in stochastic systems. *Ecology*, 97(4), p.15–1047.1. Available at: http://doi.wiley.com/10.1890/15-1047.1 [Accessed May 21, 2018].

Ozgul, A. et al., 2010. Coupled dynamics of body mass and population growth in response to environmental change. *Nature*, 466(7305), pp.482–485. Available at: http://dx.doi.org/10.1038/nature09210.

Ozgul, A. et al., 2014. Linking body mass and group dynamics in an obligate cooperative breeder A. Mysterud, ed. *Journal of Animal Ecology*, 83(6), pp.1357–1366. Available at: http://doi.wiley.com/10.1111/1365-2656.12239 [Accessed May 13, 2018].

Price, T.D., Qvarnström, A. & Irwin, D.E., 2003. The role of phenotypic plasticity in driving genetic evolution. *Proceedings of the Royal Society - Biological sciences*.

Reed, T.E. et al., 2010. Phenotypic plasticity and population viability: the importance of environmental predictability. *Proceedings. Biological sciences / The Royal Society*, 277(1699), pp.3391–400. Available at: http://rspb.royalsocietypublishing.org/content/277/1699/3391.short.

Reed, T.E., Schindler, D.E. & Waples, R.S., 2011. Efectos Interactivos de la Plasticidad Fenot??pica y Evoluc??on sobre la Persistencia Poblacional en un Clima Cambiante. *Conservation Biology*, 25(1), pp.56–63.

Robinson, J.D., Wares, J.P. & Drake, J.M., 2013. Extinction hazards in experimental Daphnia magna populations: Effects of genotype diversity and environmental variation. *Ecology and Evolution*.

Sanchez, A. & Gore, J., 2013. Feedback between Population and Evolutionary Dynamics Determines the Fate of Social Microbial Populations S. P. Ellner, ed. *PLoS Biology*, 11(4), p.e1001547. Available at: http://www.ncbi.nlm.nih.gov/pubmed/23637571 [Accessed April 24, 2018].

Scheffer et al., 2009. Early-warning signals for critical transitions. *Nature*, 461, pp.53–59. Available at: http://dx.doi.org/10.1038/nature08227%5Cn%3CGo to ISI%3E://WOS:000269478800026%5Cnhttp://www.nature.com/nature/journal/v461/n7260/pdf/nature08227.pdf.

Scheffer, M. et al., 2012. Anticipating Critical Transitions. *Science*, 338(6105), pp.344–348.

Scheffer, M. et al., 2001. Catastrophic shifts in ecosystems. *Nature*, 413(6856), pp.591–6. Available at: http://www.ncbi.nlm.nih.gov/pubmed/15448261.

Scheffer, M. et al., 2009. Early-warning signals for critical transitions. *Nature*, 461(7260), pp.53–59. Available at: http://dx.doi.org/10.1038/nature08227%5Cn%3CGo to ISI%3E://WOS:000269478800026%5Cnhttp://www.nature.com/nature/journal/v461/n7260/pdf/nature08227.pdf.

Spanbauer, T.L. et al., 2016. Body size distributions signal a regime shift in a lake ecosystem. *Proceedings of the Royal Society B*, 283, p.20160249.

Strogatz, S.H., 1994. Nonlinear Dynamics and Chaos. *Book*, pp.1–505.

Thomas, C.D. et al., 2004. Extinction risk from climate change. *Nature*, 427(6970), pp.145–8. Available at: http://www.ncbi.nlm.nih.gov/pubmed/18653892.

Villa Martín, P. et al., 2015. Eluding catastrophic shifts. *Proceedings of the National Academy of Sciences*.

Vuren, D. Van & Armitage, K.B., 1991. Duration of snow cover and its influence on life-history variation in yellow-bellied marmots. *Canadian Journal of Zoology*.

Wissel, C., 1984. A universal law of the characteristic return time near thresholds. *Oecologia*, 65(1), pp.101–107.

Yoshida, T. et al., 2003. Rapid evolution drives ecological dynamics in a predator–prey system. *Nature*.

Yvonne, W. & Hoffmann, A.A., 2009. Demographic factors and genetic variation influence population persistence under environmental change. *Journal of Evolutionary Biology*.

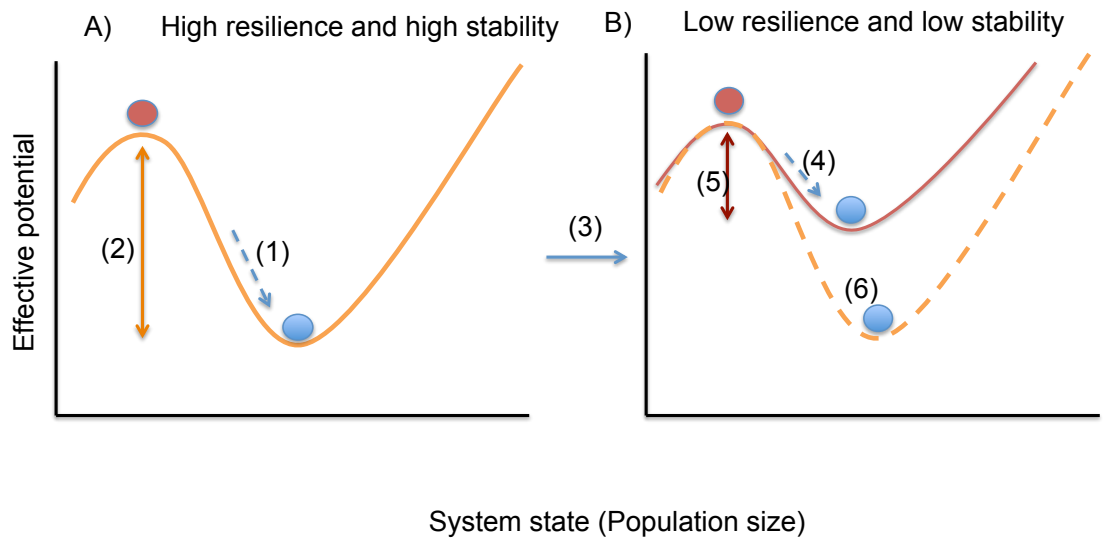

Figure 1. Illustration of the 'ball-in-cup' potential energy curve in relation to stability and resilience of a one-dimensional dynamical system. The stable state of the dynamical system in this illustration is indicated by the blue ball, and the unstable state (or the tipping point) is indicated by the red ball in both A and B. (1) shows that the slope of the potential curve (i.e., stability) is steep and the basin where the ball lies is also deep signifying that both resilience as well as stability is high. This means that the amount of potential energy (2) to push the ball from its stable state (blue) to the unstable state (red) or in other words the loss in stability will be large. However, due to changes in ecological or evolutionary factors intrinsic to the dynamical system (3), the 'ball-in-cup' potential energy curve can shift from (6) to (4) where the slope is now less steep, signifying a loss in stability. Along with this, there is also a loss in resilience. Now, the amount of potential energy (5) to move the blue ball at (4) to the unstable state for (B) is less. This could reflect in the strength of EWS of population collapse.

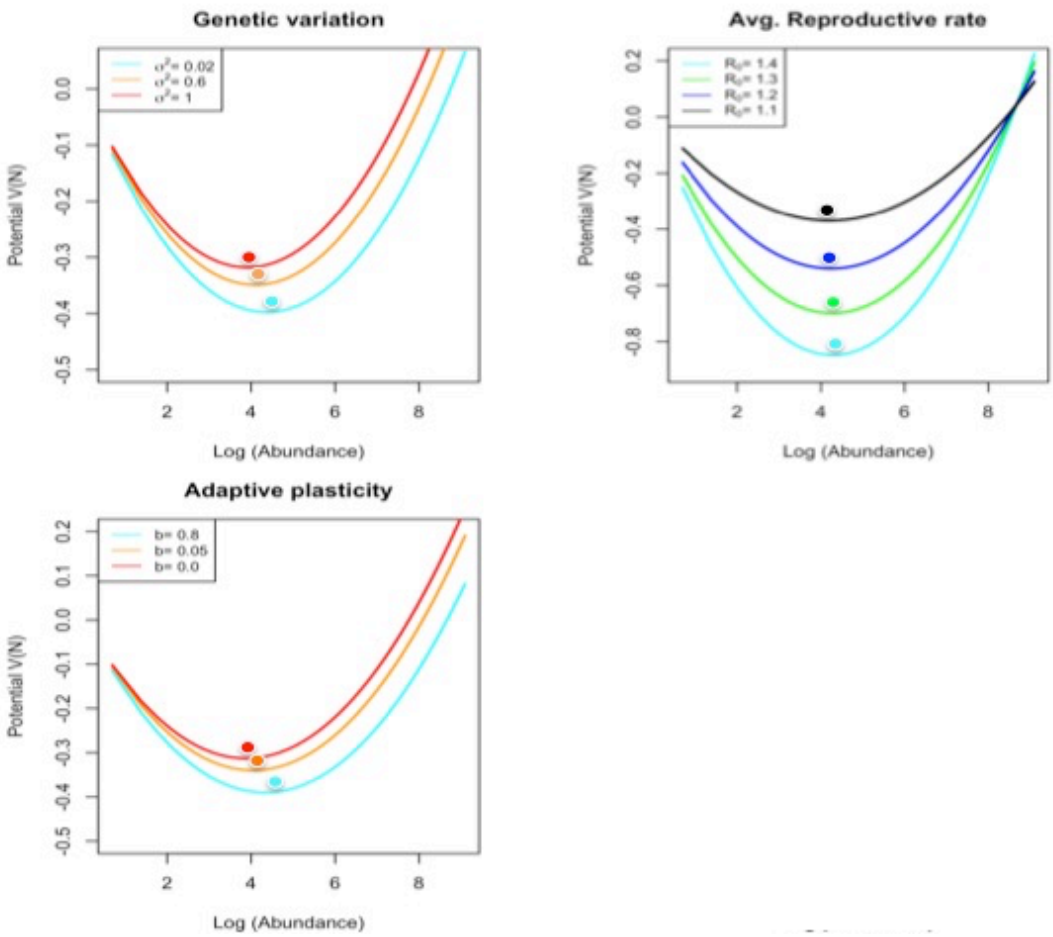

Figure 2. Effective potential $V(N)$ plotted as a function of the state variable abundance, N. Note the effective potential is altered by factors like genetic variation, adaptive plasticity and net reproductive rate. The lower the value of the effective potential, more stable the system is.

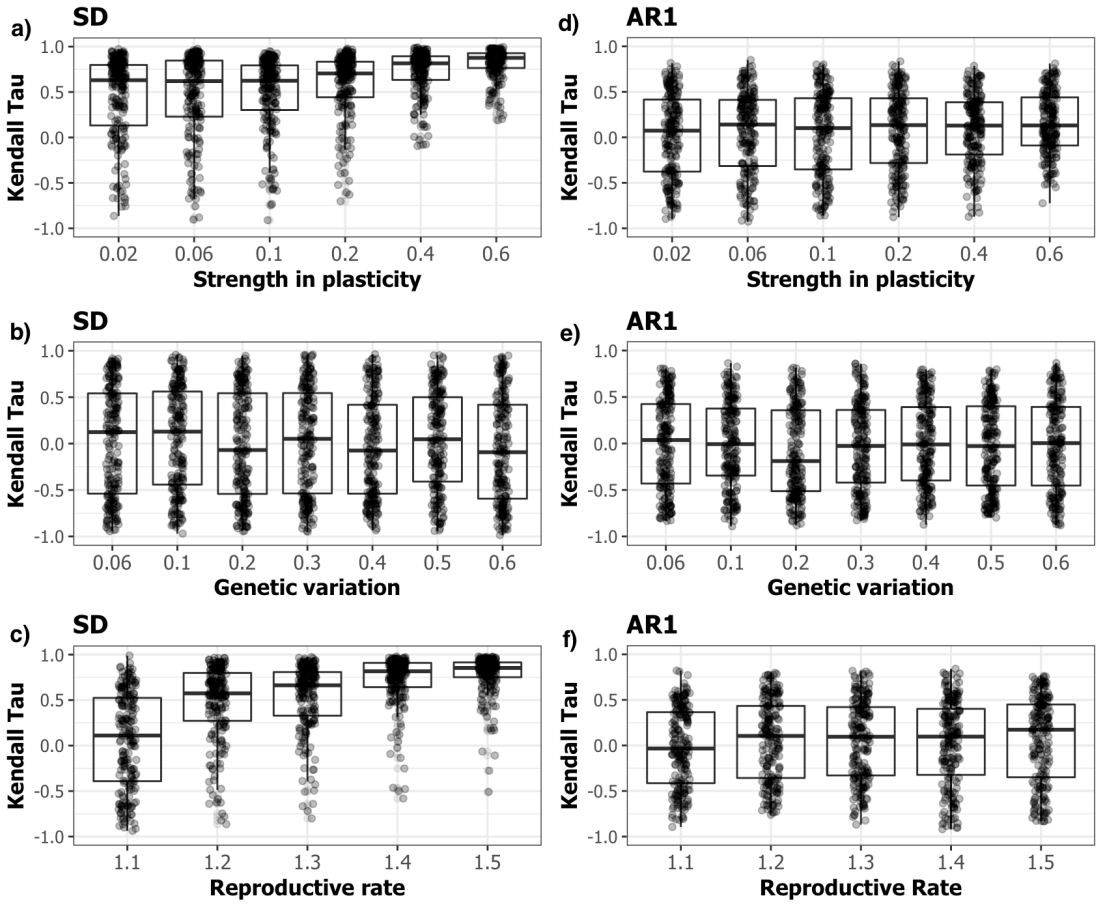

Figure 3. Box plots showing the distribution of Kendall's Tau correlation coefficient (high values around 0.7 are usually considered an EWS) for 200 simulation of population collapse for different levels of adaptive plasticity *b,* genetic variation σ_a^2, reproductive rate R_0. The leading indicators that are shown here are autocorrelation at lag-1 (AR1) and standard deviation (SD). X-axis is the different levels of the above factors.

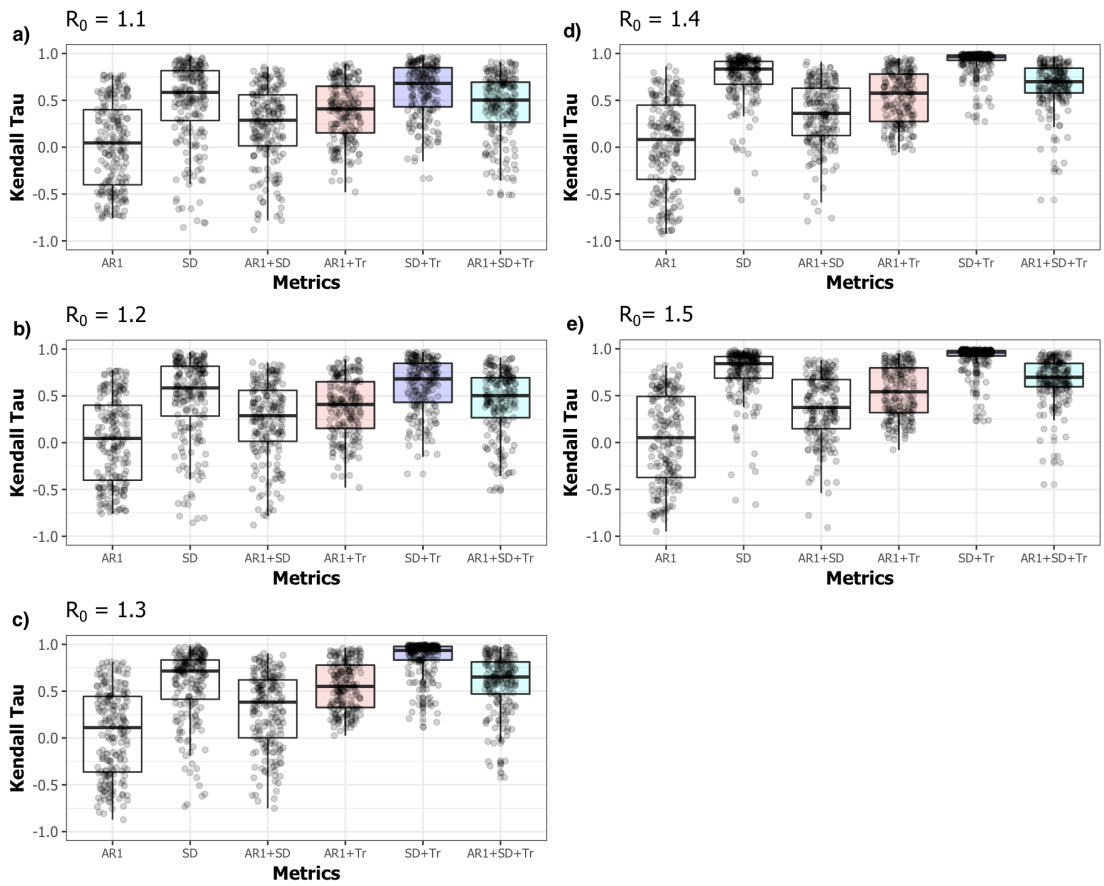

Figure 4. Box plots showing the distribution of Kendall's Tau correlation coefficient for 200 simulation of population collapse for different levels of net reproductive rate R_0. On the X-axis are the different early warning metrics shown : autocorrelation at lag-1 (AR1), standard deviation (SD), (*AR1+SD*),(*AR1+Tr*), (*SD+Tr*) ,(*AR1+SD+Tr*). *Tr* corresponds to the mean value of the phenotypic trait. Colored boxplots denote the trait-based EWS while white boxplots denote abundance-based EWS.